Vibration Suppression Control of Space Flexible Manipulator with Varying Load Based on Adaptive Neural Network

Jinmiao Shen, Wenhui Zhang, Shuhua Zhou, and Xiaoping Ye

***Abstract*—A neural network control method for terminal load identification is designed to solve the variable load problem of the space robot terminal. The space robot model is decomposed into two dynamic sub models by singular perturbation theory: rigid and flexible Considering the influence of variable load mass on the dynamic model, a weighted recursive least squares method (WRLSM) is designed to identify the estimation of unknown quality. The uncertain model error is compensated by neural network. Aiming at the problem of elastic vibration caused by flexible characteristics, a linear quadratic regulator (LQR) strategy is designed to suppress the chattering of robot flexible arm. Simulation verifies the effectiveness of the controller.**

***Index Terms*—Space flexible manipulator; Variable load; Quality estimation; Adaptive control; Neural network; Vibration suppression.**

I. Introduction

COMPARED with rigid manipulator, flexible manipulator has lighter weight, higher speed and lower energy consumption [1], so it has been widely used in space technology. From the earlier Canadian canadarm-2 space manipulator of the European Union "International Space Station" to the large space manipulator of the Chinese "Tiangong 1" space station, Manipulator made of flexible composite material, which makes the space manipulator show strong flexibility. This flexibility can better absorb the impact energy generated when the robot collides with other objects. However, the flexible characteristics will make the robot chatter in the process of motion [2-4], which will seriously affect the high accuracy of the robot terminal. Moreover, robots will have more difficult tasks in space, such as cleaning up space garbage or capturing unknown targets [5-7], the target load quality is unknown. If the difference between the captured target load and the preset load is too large, it is easy to cause load mutation, which will damage the stability of the actuator [8-9]. Therefore, the research of space flexible arm control based on non-cooperative target acquisition has important practical significance.

In recent years, few international scholars have studied the problem of non-cooperative target load acquisition, but they have proposed different control strategies for robot control, such as sliding mode [10-12], adaptive [13,14], neural network [15,16], robust [17]. There have also made some meaningful research results on the space flexible arm robot with varying load [18-23].

Lei et al. [24] proposed a fault-tolerant control tactics by neural network for floating space flexible robot, and a quadratic optimal controller to suppress elastic vibration. Chen et al. [25] proposed an active disturbance rejection control (ADRC) tactics for the single flexible arm with disturbance. The state observer is designed to estimate the disturbance, and the feedback controller is designed to compensate the disturbance. Hamzeh et al. [26] proposed a composite control tactics based on sliding mode for a single arm, in which one controller realizes position tracking and the other controller suppresses elastic vibration. Lei et al. [27] proposed an adaptive control method based on $H\infty$ for free floating space flexible robot, and designed a robust controller based on $H\infty$ to track the desired trajectory, and devised an adaptive controller based on optimal control theory to suppress elastic vibration.

At present, scholars at home and abroad mainly focus on the flexible arm without considering the load change, but the research on variable load target is relatively few. In fact, considering the complex task conditions of the space robot, such as cleaning up space garbage or capturing unknown targets, the target load quality is unknown. If load is too large, it is easy damage the stability of the control system.

Through the above analysis, a neural network control tactics based on calculated torque is devised. The purpose of the controller is to estimate the unknown load mass, and realize the complete decoupling of the unknown nonlinear model, and suppress the elastic vibration. The main innovation points are as follows.

1) Different from the traditional control, which controls the robot dynamics model as a whole, this research decomposes dynamics model into two dynamics subsystem models to realize the separate control of the two subsystems;

2) Different from the traditional control object which is a constant mass load, the recursive weighted least squares

Manuscript received October 6, 2022; revised February 27, 2023.

This work was supported by the National Natural Science Foundation of China (61772247), Key projects of Natural Science Foundation of Zhejiang Province (LZ21F020003), the National Natural Science Foundation of Zhejiang Province (LY20E050002, LY18F030001) and Nanjing Xiaozhuang College Talent Fund (2020 NXY14).

Jinmiao Shen is a postgraduate student of Machinery and Automatic Control, Zhejiang Sci-Tech University, Hangzhou 310000, China. (e-mail: sjm1053314262@163.com).

Wenhui Zhang is a professor of electronic engineering, Nanjing Xiaozhuang University, Nanjing 211171, China. (corresponding author to provide phone: 02586178619; e-mail: zwh1484443882@163.com).

Shuhua Zhou is a professor of Zhejiang Technical Institute of Economics, Hangzhou 310000, China. (e-mail: Mj_zwh@126.com).

Xiaoping Ye is a professor of the College of Technology, Lishui University, Lishui 323000, China. (e-mail: hit_qnm@126.com).

method is devised to discriminate identification of the variable mass load;

3) Different from the partial decoupling of nonlinear model in traditional control, an adaptive controller based on neural network is designed to realize compensation control, so as to realize complete decoupling of nonlinear model. At the same time, a LQR controller is devised to suppress the elastic vibration.

II. Dynamic Modeling of Floating Space Flexible Manipulator

From Fig. 1, the free-floating space flexible robot is composed of carrier B_0 , flexible rods B_1 and B_2 . The joint system $B_i(i=0,1,2)$ of each split $O_i x_i y_i$ is established. The load mass p is m , and the specific parameters are defined in references [24,28].

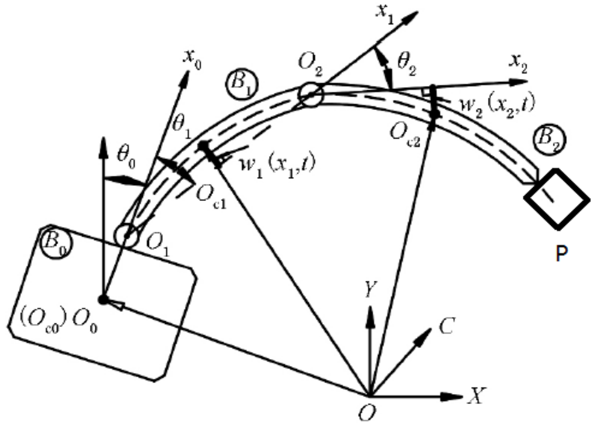

Fig. 1. Two-bar flexible space robot system

Assuming that the flexible arm with two degrees of freedom is a slender homogeneous arm, if rod B_1 is regarded as a simply supported beam and rod B_2 as a cantilever beam, it is a Bernoulli Euler beam [25]. Here, bending deformation is mainly considered. Shear deformation is ignored. If the bending rigidity of the section is $(EI)_i$ and the linear density of the flexible rod $B_i(i=1,2)$ is ρ_i , its elastic deformation is recorded as

$$u_i(x_i,t)=\sum_{i=1}^{\infty}\phi_{ij}(x_i)q_{ij}(t) \tag{1}$$

Where $u_i(x_i,t)$ is the transverse elastic deformation of B_i at section $x_i(0\le x_i\le l_i)$. $\phi_{ij}(x_i)$ is the j order modal function of B_i. The specific modal function is referred to [28]. $q_{ij}(t)$ is the modal coordinate corresponding to $\phi_{ij}(x_i)$. n_i is the number of truncation terms. where the first two modes are taken as $i=1,2$.

Based on the Lagrange equation of the second kind and the momentum conservation theorem, the dynamic equation of the flexible robot can be obtained as follows and the detailed calculation process is shown in [31]:

$$M(\theta_b,q)\begin{bmatrix}\ddot{\theta}\\ \ddot{q}\end{bmatrix}+H(\theta_b,\dot{\theta},q,\dot{q})\begin{bmatrix}\dot{\theta}\\ \dot{q}\end{bmatrix}+\begin{bmatrix}\xi\\ Kq\end{bmatrix}=\begin{bmatrix}\tau\\ 0\end{bmatrix} \tag{2}$$

Where $\theta_b=[\theta_0,\theta]^T$, $\theta=[\theta_1,\theta_2]^T$ and and θ is the rigid generalized coordinate column vectors of the joint angle of the arm. $q=[q_{11}\quad q_{12}\quad q_{21}\quad q_{22}]^T$ is the flexible generalized coordinate column vector of the flexible modal coordinates of the member. $H(\theta_b,\dot{\theta},q,\dot{q})$ is column vector containing Coriolis force and centrifugal force. $K=\mathrm{diag}(k_{11},k_{12},k_{21},k_{22})$ is the stiffness matrix of the member, $k_{ij}=(EI)_i\int_0^{li}(\phi_{ij}^{''})^T\phi_{ij}^{''}dx_i$. $\tau=[\tau_1\quad \tau_2]^T$ is the output torque of the rod joint, and ξ is the external interference and joint friction.

Writing (2) as a block matrix in the form of

$$\begin{bmatrix}M_{rr} & M_{rf}\\ M_{fr} & M_{ff}\end{bmatrix}\begin{bmatrix}\ddot{\theta}\\ \ddot{q}\end{bmatrix}+\begin{bmatrix}H_{rr} & H_{rf}\\ H_{fr} & H_{ff}\end{bmatrix}\begin{bmatrix}\dot{\theta}\\ \dot{q}\end{bmatrix}+\begin{bmatrix}\xi\\ Kq\end{bmatrix}=\begin{bmatrix}\tau\\ 0\end{bmatrix} \tag{3}$$

Where $M_{rr}\in\mathbb{R}^{2\times2}$, $M_{fr}=M_{fr}^T\in\mathbb{R}^{2\times4}$, $M_{ff}\in\mathbb{R}^{4\times4}$, $H_{\mathrm{rr}}\in\mathbb{R}^{2\times2}$, $H_{ff}\in\mathbb{R}^{4\times4}$, $H_{fr}\in\mathbb{R}^{4\times2}$, $H_{rf}\in\mathbb{R}^{2\times4}$.

$M(\theta_b,q)$ inverse is

$$N^{-1}=M=\begin{bmatrix}M_{rr} & M_{rf}\\ M_{fr} & M_{ff}\end{bmatrix}^{-1}=\begin{bmatrix}N_{rr} & N_{rf}\\ N_{fr} & N_{ff}\end{bmatrix} \tag{4}$$

If the singular perturbation scale factor is defined as $\mu=(\min(k_{11},k_{12},k_{21},k_{22}))^{-1/2}$, and the state variable is defined as $z=q/\mu^2$, and the new stiffness matrix is defined as $\tilde{K}=\mu^2K$, then (3) can be decomposed into and characterized as a fast subsystem with flexible characteristics:

$$\begin{aligned}\ddot{\theta}=&-(N_{rr}H_{rr}+N_{rf}H_{fr})-(N_{rr}H_{rf}\\ &+N_{rf}H_{ff})\mu^2\dot{z}-N_{rf}\tilde{K}z+N_{rr}(\tau-\xi)\end{aligned} \tag{5}$$

$$\begin{aligned}\mu^2\ddot{z}=&-(N_{fr}H_{rr}+N_{ff}H_{fr})\dot{\theta}-(N_{fr}H_{rf}+\\ &N_{ff}H_{fr})\mu^2\dot{z}-N_{ff}\tilde{K}z+N_{fr}(\tau-\xi)\end{aligned} \tag{6}$$

The design master controller is

$$\tau=\overline{\tau}+\tau_f \tag{7}$$

Where $\overline{\tau}$ is a slowly varying subsystem controller, which is used to track the desired trajectory. τ_f is a fast-changing subsystem controller, which is used to suppress elastic vibration.

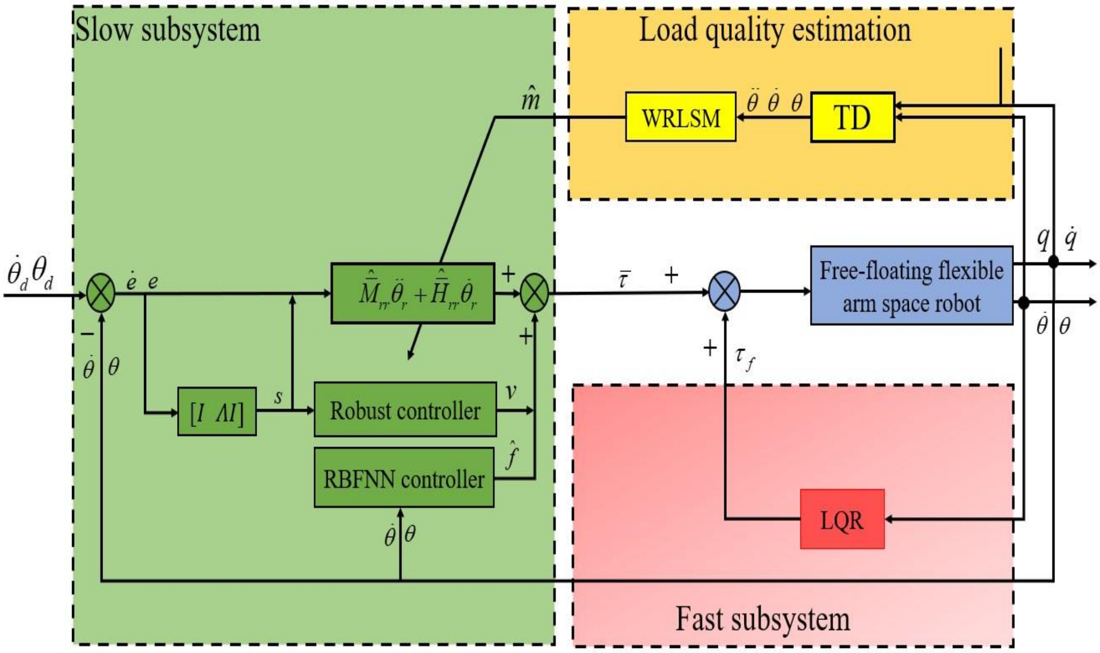

Fig. 2. Control technology road map

In order to obtain the slowly varying subsystem model representing the rigid characteristics, letting $\mu = 0$ be substituted into equation (6) to sort out the slowly varying manifold expression $\bar{z}$:

$$\bar{z} = \tilde{K}^{-1}\bar{N}_{ff}^{-1}[-(\bar{N}_{fr}\bar{H}_{rr} + \bar{N}_{ff}\bar{H}_{fr})\dot{\theta} + \bar{N}_{fr}(\bar{\tau} - \xi)] \quad (8)$$

Where the superscript "-" represents the physical quantity of the slowly varying subsystem. Then, substituting (8) into (7) and combining with $\bar{M}_{rr}^{-1} = \bar{N}_{rr} - \bar{N}_{rf}\bar{N}_{ff}\bar{N}_{rf}$, the slowly varying subsystem is obtained as follows:

$$\bar{M}_{rr}\ddot{\theta} + \bar{H}_{rr}\dot{\theta} + \xi = \bar{\tau} \quad (9)$$

In order to obtain the fast-varying subsystem model that characterizes the flexibility, the time scale of the fast-varying subsystem $p_1 = z - \bar{z}, p_2 = \mu\dot{z}$ is set as $\varpi = t/\mu$ and t as time. Let $\mu = 0$ be carried into (6) to sort out the expression of fast-changing manifold:

$$\frac{dp_1}{d\varpi} = p_2 \quad (10)$$

$$\frac{dp_2}{d\varpi^2} = -\bar{N}_{ff}\tilde{K}p_1 + \bar{N}_{fr}\tau_f \quad (11)$$

III. Design of Robust Compensation Controller Based on Adaptive Neural Network

Figure 2 is the flow chart of the design control system for the space flexible robot.

A. *Unknown load quality estimation*

Considering the unknown and uncertainty of the end load mass, the model items containing the load mass is decomposed into:

$$\bar{M}_{rr}(\theta_b) = M_0(\theta_b) + C_m(\theta_b)\hat{m} \quad (12)$$

$$\bar{H}_{rr}(\theta_b, \dot{\theta}) = H_0(\theta_b, \dot{\theta}) + C_H(\theta_b, \dot{\theta})\hat{m} \quad (13)$$

Where $M_0(\theta_b)$ and $H_0(\theta_b, \dot{\theta})$ are known deterministic models. $C_m(\theta_b)m$, $C_H(\theta_b, \dot{\theta})m$ are unknown uncertain models.

Substituting (12) and (13) into (2) to obtain

$$\phi^T\hat{m} = \eta \quad (14)$$

Where

$\phi^T = C_m(\theta_b)\ddot{\theta} + C_H(\theta_b, \dot{\theta})\dot{\theta}$;

$\eta = \bar{\tau} - d - M_0(\theta_b)\ddot{\theta} - H_0(\theta_b, \dot{\theta})\dot{\theta}$.

Assuming that the actual quality of the load is m and the estimated quality is $\hat{m}$, the quality estimator is designed based on the improved weighted recursive least square method (WRLSM):

$$\hat{m}_k = \hat{m}_{k-1} + K_k(\eta_k - \phi_k^T\hat{m}_{k-1}) \quad (15)$$

$$N_k = N_{k-1} - N_{k-1}\phi_k(L_k + \phi_k^T N_{k-1}\phi_k)^{-1}\phi_k^T N_{k-1} \quad (16)$$

$$K_k = N_{k-1} - \phi_k(L_k + \phi_k^T N_{k-1}\phi_k)^{-1} \quad (17)$$

Where $\eta_k - \phi_k^T\hat{m}_{k-1}$ is the prediction error. K_k is the gain matrix. L_k is the weighting matrix.

According to (14), the designed quality estimator needs to know the angular acceleration signal. The higher-order differential of the angular position signal. Then the tracking differentiator (TD) is designed as:

$$\begin{cases} \dot{x}_1 = x_2 \\ \dot{x}_2 = h(x_1 - \bar{\tau}, x_2, r, h_0) \end{cases} \quad (18)$$

Where $x_1 = \theta$ and h_0 are filter factors. r are velocity factors. $\bar{\tau}$ are torque output.

Design the function of $h(x_1 - \bar{\tau}, x_2, r, h_0)$ as

$$\begin{cases} h = -r\,\mathrm{sgn}(a) & |a| > d_0 \\ h = -ra/d & |a| \le d_0 \end{cases} \tag{19}$$

Where

$$a = \begin{cases} x_2 + 0.5(a_0 - d)\,\mathrm{sgn}(y) & |y| > d_0 \\ x_2 + y/h_0 & |y| \le d_0 \end{cases}, \quad d_0 = h_0 d \quad ,$$

$a_0 = \sqrt{d^2 + 8r|y|}$, $d = rh_0$, $y = x_1 + h_0 x_2$.

B. Neural network control design

Defining the sliding surface as:

$$s = \dot{e} + \Lambda e \tag{20}$$

Where Λ is positive matrix. $e = \theta - \theta_d$ is position error. θ_d is ideal angle. $\dot{e}$ is velocity error. Defining reference input as θ_r, then

$$\dot{\theta}_r = \dot{\theta}_d - \Lambda e \tag{21}$$

Combing (18) - (19) can obtain

$$s = \dot{\theta} - \dot{\theta}_r \tag{22}$$

In order to prove the stability of the system, the following functions are constructed

$$V(t) = \frac{1}{2} s^T \bar{M}_{rr} s \tag{23}$$

Differentiate the above equation

$$\begin{aligned} \dot{V}(t) &= s^T \bar{M}_{rr} \dot{s} + \frac{1}{2} s^T \bar{M}_{rr} s \\ &= -s^T [\bar{M}_{rr} \ddot{\theta}_r + \bar{H}_{rr} \dot{\theta}_r + \xi - \bar{\tau}] \end{aligned} \tag{24}$$

Assuming that models $\bar{M}_{rr}$ and $\bar{H}_{rr}$ are accurately known. ξ is also accurately known. The following control law can be devise as

$$\bar{\tau}^1 = \bar{M}_{rr} \ddot{\theta}_r + \bar{H}_{rr} \dot{\theta}_r + \xi - K_v s \tag{25}$$

Where K_v is a positive matrix. If (25) is brought into (24), getting

$$\dot{V}(t) = -s^T K_v s \le 0 \tag{26}$$

However, in the actual project, $\xi \ne 0$, and the designed load quality estimator must have some identification errors. Especially in the initial stage, there are few sample data, and there are large identification errors. With the iteration of online data samples, the identification accuracy will gradually improve. Letting the quality identification error be $\Delta m = m - \hat{m}$, and from (12) - (13), the model error is

$$\Delta \bar{M}_{rr}(\theta_b) = \bar{M}_{rr} - \hat{\bar{M}}_{rr} = C_m(\theta_b)\Delta m \tag{27}$$

$$\Delta \bar{H}_{rr}(\theta_b, \dot{\theta}) = \bar{H}_{rr} - \hat{\bar{H}}_{rr} = C_H(\theta_b, \dot{\theta})\Delta m \tag{28}$$

Where the dynamic estimation models with load estimation mass $\hat{m}$ are defined as $\hat{\bar{M}}_{rr}$ and $\hat{\bar{H}}_{rr}$ respectively. The error models caused by load quality estimation errors are $\Delta \bar{M}_{rr}$ and $\Delta \bar{H}_{rr}$.

Bringing (27) - (28) into the controller (23), and considering the existence of external interference and other uncertain factors, $\xi \ne 0$. Then the new controller is designed as:

$$\bar{\tau}^2 = \hat{\bar{M}}_{rr} \ddot{\theta}_r + \hat{\bar{H}}_{rr} \dot{\theta}_r + f - K_v s \tag{29}$$

$$f = \Delta \bar{M}_{rr} \ddot{\theta}_r + \Delta \bar{H}_{rr} \dot{\theta}_r + \xi \tag{30}$$

If f can be accurately obtained, Then the function can be composed as follows

$$V(t) = \frac{1}{2} s^T \bar{M}_{rr} s$$

Differentiate the above equation

$$\begin{aligned} \dot{V}(t) &= s^T \bar{M}_{rr} \dot{s} + \frac{1}{2} s^T \bar{M}_{rr} s \\ &= -s^T [\bar{M}_{rr} \ddot{\theta}_r + \bar{H}_{rr} \dot{\theta}_r + \xi - \tau_{zs}^2] \\ &= -s^T K_v s \le 0 \end{aligned} \tag{31}$$

Then the control system is stable.

However, since f is an uncertain nonlinear function, it needs to be compensated. Considering that the neural network has good nonlinear compensation ability and is widely involved in the field of motion control, the neural network is used for compensation [29, 30].

RBF neural network f optimal output is

$$f(x) = W^{*T} \varphi(x) + \varepsilon \tag{32}$$

Where $x = (\theta_0, \theta_1, \theta_2)$ is the input. W^* is the weight matrix. ε is the approximation error. $\varphi(x)$ is a Gaussian function.

According to the learning characteristics of neural network, the following assumptions are made:

Assumption 1: The optimal weight parameter W^*, that is, there is a normal number W_M, which satisfies $\|W^*\| \le W_M$ and there is any small positive number ε_M, so that the neural network approximation error ε can meet $|\varepsilon| < \varepsilon_M$.

If actual output is $\hat{f}$,

$$\hat{f} = \hat{W}^T \varphi \tag{33}$$

Where $\hat{W}$ is the actual weight.

From (32) and (33), It can be concluded that

$$\Delta\hat{f} = f - \hat{f} = W^{*\mathrm{T}}\varphi + \varepsilon - \hat{W}^{\mathrm{T}}\varphi = \tilde{W}^{\mathrm{T}}\varphi + \varepsilon \tag{34}$$

Where $\tilde{W}=W^* - \hat{W}$.

In order to eliminate the influence of error $\Delta\hat{f}$, a robust controller τ_v is designed here to increase the stability of the system, and the control law (31) is rewritten as

$$\bar{\tau}^3 = \hat{\bar{M}}_{rr}\ddot{\theta}_r + \hat{\bar{H}}_{rr}\dot{\theta}_r + \hat{f} - K_v s - \tau_v \tag{35}$$

$$\tau_v = \varepsilon_M \operatorname{sgn}(s) \tag{36}$$

The weight adaptive law is devised as

$$\dot{\hat{W}} = -\gamma_0 \varphi s^T \tag{37}$$

Where γ_0 is positive matrix.

Theorem: for the space robot formula (9), the control formula (35), formula (33), formula (37) and formula (36) can ensure the global asymptotic stability.

Proof: defining function

$$V = \frac{1}{2}s^T \hat{\bar{M}}_{rr} s + \frac{1}{2}tr(\tilde{W}^T \gamma_0^{-1}\tilde{W}) \tag{38}$$

Differentiate the above equation

$$\dot{V}(t) = -s^T[\Delta\hat{\bar{M}}_{rr}\ddot{\theta}_r + \Delta\hat{\bar{H}}_{rr}\dot{\theta}_r + \hat{f} + K_v s + \varepsilon_M \operatorname{sgn}(s)] + tr(\tilde{W}^T \gamma_0^{-1}\dot{\tilde{W}}) \tag{39}$$

Substituting (34) and (35) into (39), getting

$$\begin{aligned}\dot{V} &= -s^T[f - \hat{f} - K_v s - \varepsilon_M \operatorname{sgn}(s)] + tr(\tilde{W}^T \gamma_0^{-1}\dot{\tilde{W}}) \\ &= -s^T K_v s - s^T[\varepsilon + \varepsilon_M \operatorname{sgn}(s)] + tr\tilde{W}^T(\gamma_0^{-1}\dot{\tilde{W}} + \varphi s^T)\end{aligned} \tag{40}$$

Substituting (37) into (40), after simplification, getting:

$$\dot{V} = -s^T K_v s - s^T(\varepsilon_M \operatorname{sgn}(s) + \varepsilon) \le -s^T K_v s \tag{41}$$

Since K_v is a positive definite symmetric matrix

$$\dot{V} \le 0 \tag{42}$$

Then the system will finally be in a stable state.

C. Quick change subsystem LQR controller

Writing (10) ~ (11) in the form of state space, and making $L = \begin{bmatrix} p_1 \\ p_2 \end{bmatrix}$ state variable, which express as:

$$\dot{L} = A_f L + B_f \tau_f \tag{43}$$

Where $A_f = [\begin{matrix} 0 & I \\ -\bar{N}_{ff}\tilde{K} & 0 \end{matrix}]$. $B_f = \begin{bmatrix} 0 \\ \bar{N}_{fr} \end{bmatrix}$.

The optimal control technology is adopted for vibration suppression. The objective function is selected as

$$J = \frac{1}{2}\int_0^\infty (L^T Q L + \tau_f^T R \tau_f)dt \tag{44}$$

Where Q and R are weight coefficient matrices. If the standard LQR design is adopted, the control output is

$$\tau_f = -KL \tag{45}$$

Where $K = -R^{-1}B^T P(t)$.

P by satisfying Riccati equation:

$$\dot{P}(t) = -P(t)A_f - A_f^T P(t) + P(t)BR^{-1}B^T P(t) - Q \tag{46}$$

IV. Experimental simulation

Taking the dynamic model given in Fig. 1 as an example. Combined with the load estimation (16) - (18), the simulation is carried out by using formula (23) and formula (44). The parameters of the floating space flexible manipulator are as follows:

$l_0 = l_1 = 2m$, $l_2 = 2.5m$, $m_0 = 40kg$, $m_1 = 5kg$, $m_2 = 2.5kg$, $J_0 = 35kg \cdot m^2$, $\rho_1 = 4kg/m$, $\rho_2 = 1.2kg/m$, $(EI_1) = 50N \cdot m^2$, $(EI_2) = 50N \cdot m^2$.

The trajectory of the manipulator is:

$q_d = [\cos 0.2\pi t \;\; 1 + \sin 0.2\pi t]^T$

TD parameters are:

$r_{11} = r_{12} = 3200$, $h_{110} = h_{120} = 0.04$, $r_{21} = 1500$, $r_{22} = 2000$, $h_{210} = 0.03$, $h_{220} = 0.04$.

The controller parameters are:

$\varepsilon_{cM} = 0.05$, $\Lambda = \operatorname{diag}\{5,5\}$, $K_v = \operatorname{diag}\{10,10\}$

The weight coefficient matrix of LQR is selected as:

$Q = diag[100,10,10,10,10,10,10,10]$

$R = \operatorname{diag}[100,10]$

Uncertain nonlinear term is:

$\xi = [q_1\dot{q}_1 0.3\sin t , \;\; q_2\dot{q}_2 0.3\sin t]^T$

Initial value:

$\theta_0 = 0$, $q_1(0) = \theta_1(0) = 0$, $q_2(0) = \theta_2(0) = 0$.

The number of hidden neurons is $n = 25$ .The initial weights of the network is 0. The width of basis function and the center of the basis function is randomly designated within (0 ~ 0.1).

A. Mass identification of end load and error value of neural network

The initial parameter of the WRLSM quality estimator is $N_0 = 2000$ and $\hat{m}$ is the estimated load mass. The given initial mass is $1kg$ and the real mass is set to $6kg$. At this time, $\Delta M = 2m_2 = 5kg$ is twice the mass of arm 2. The end load identification is shown in Fig. 3.

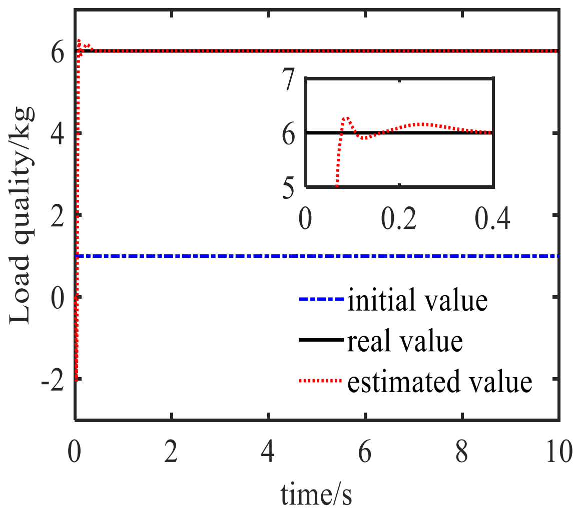

Fig.3. Load quality identification

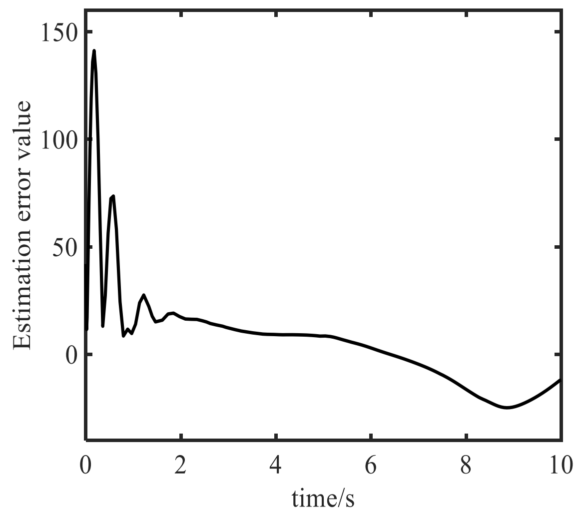

Fig.5. Estimation error value of neural network

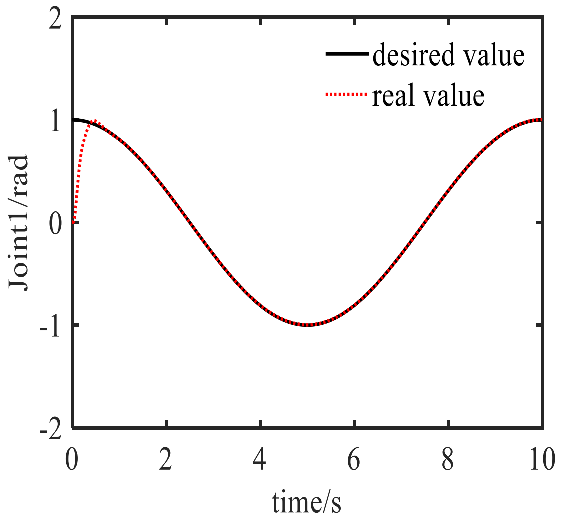

Fig.4. Joint1 angle position tracking (W-ANN)

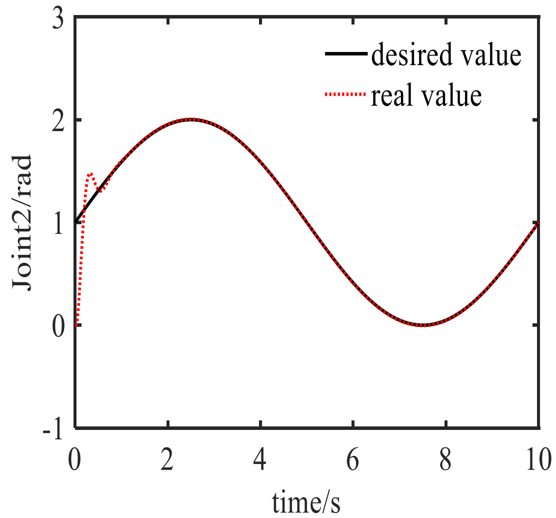

Fig.6. Joint2 angle position tracking (W-ANN)

From Fig.3, when the error of the initial value of load quality is relatively large, the quality estimator quickly tracks the real value in less than 0.5s. The overshoot is small. This shows that the designed WRLSM quality estimator is effective and can accurately estimate the unknown quality when the initial quality error is large. From Fig. 5 that the error is very large at the beginning. After 2.5s, it can better compensate the nonlinear term.

B. Neural network adaptive control of variable load

To verify the effectiveness of the adaptive neural network (ANN) control tactics and the impact of WRLSM quality estimator on the control effect. W-ANN represents the ANN algorithm using WRLSM quality estimator. ANN represents the control algorithm without WRLSM quality estimator.

a) Unknown load small range uncertainty $\Delta M = 0.5kg$

When the uncertainty of the end load is small, such as $\Delta M = 0.2m_2 = 0.5kg$, control algorithm is verified. Fig. 4,6 is the joint angle trajectory tracking diagram using W-ANN algorithm. Fig. 7,10 is the first-order modal diagram of the arm using W-ANN algorithm. Fig. 8,11 is the joint angle trajectory tracking diagram using ANN algorithm. Fig. 9,12 is the first-order modal diagram of the arm using ANN algorithm.

From Fig. 4,6 and Fig. 8,11, when the load uncertainty is $\Delta M = 0.2m_2 = 0.5kg$,the proposed W-ANN algorithm or ANN algorithm can accurately track the actual trajectory within about 1s. Due to the small uncertainty of load, the control effect achieved by using W-ANN algorithm or ANN algorithm is similar, which shows that the designed ANN controller has good robustness and can realize better compensation control for model mutation caused by small load change. In the case of small load uncertainty, From Fig.7,10 and Fig. 9,12 that the first-order modal shape of the flexible arm is not violent.

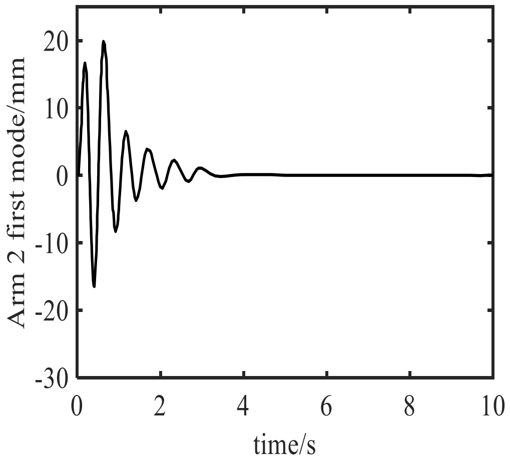

Fig.7. First order mode of flexible arm1 (W-ANN)

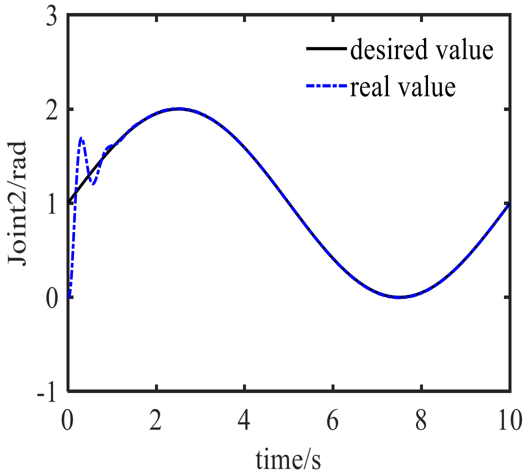

Fig.8. Joint1 angle position tracking (ANN)

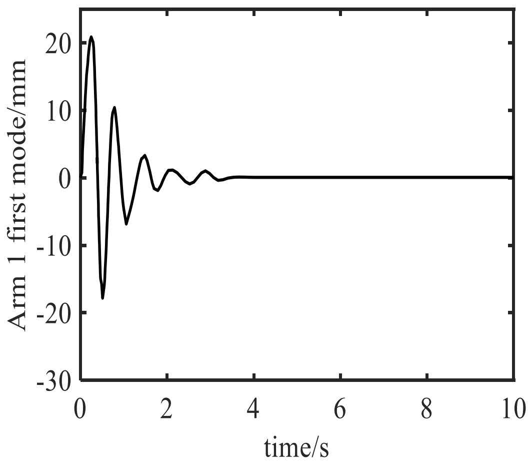

Fig.9. First order mode of flexible arm1 (ANN)

C. Unknown load large range uncertainty $\Delta M = 5kg$

When the uncertainty of the end load is large, such as $\Delta M = 2m_2 = 5kg$, the change of the end load is twice the mass of the boom, and control tactics is verified. Fig.13,16 is the joint angle trajectory tracking diagram using W-ANN

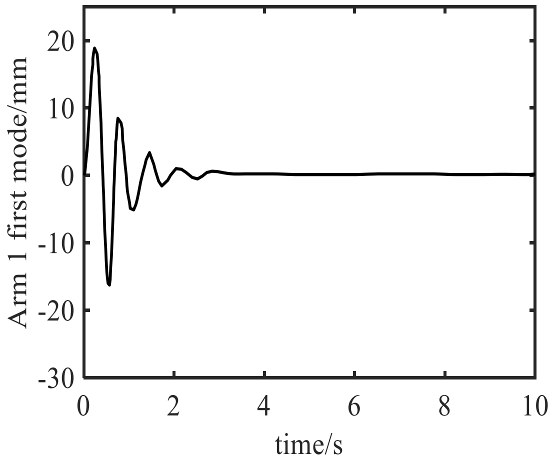

Fig.10. First order mode of flexible arm2 (W-ANN)

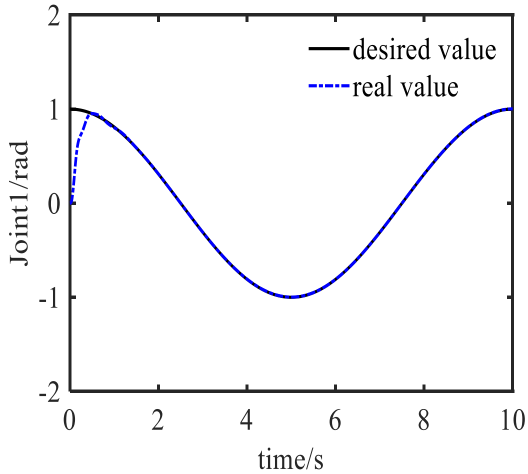

Fig.11. Joint2 angle position tracking (ANN)

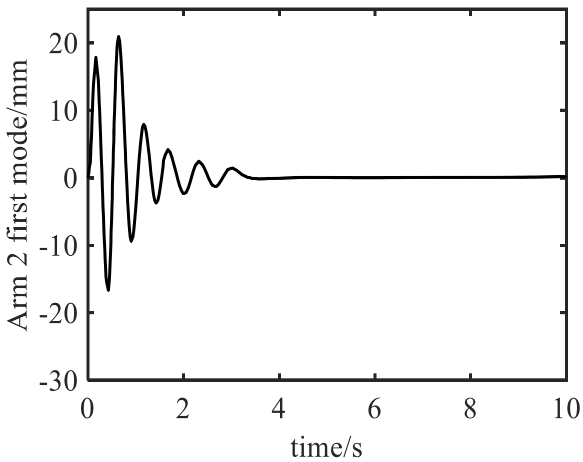

Fig.12. First order mode of flexible arm2 (ANN)

algorithm. Fig.14,17 is the first-order modal diagram of the arm using W-ANN algorithm. Fig.15,18 is the joint angle trajectory tracking diagram using ANN algorithm. Fig.19,22 is the first-order modal diagram of the arm using ANN algorithm.

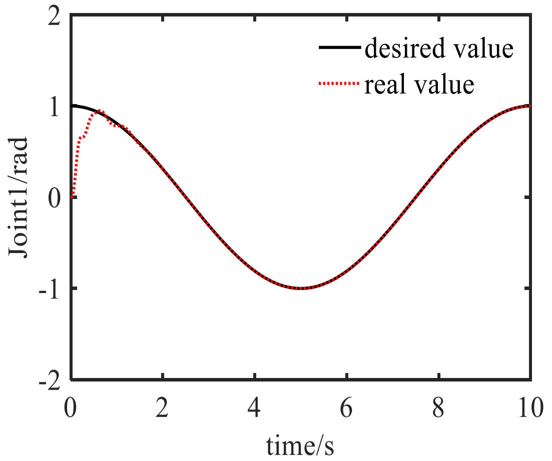

Fig.13. Joint1 angle position tracking (W-ANN)

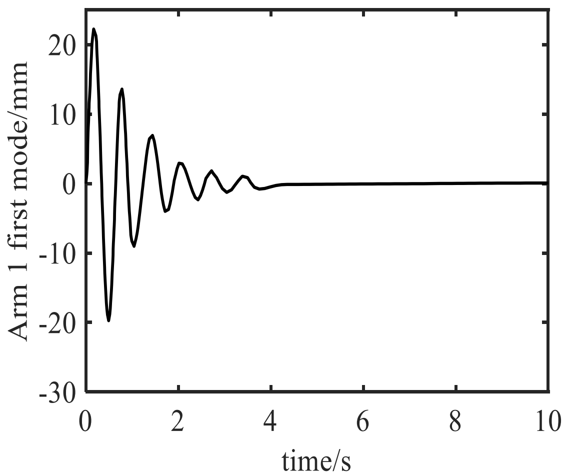

Fig.14. First order mode of flexible arm1 (W-ANN)

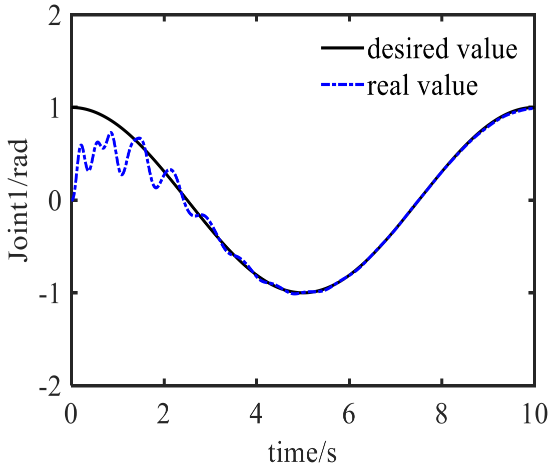

Fig.15. Joint1 angle position tracking (ANN)

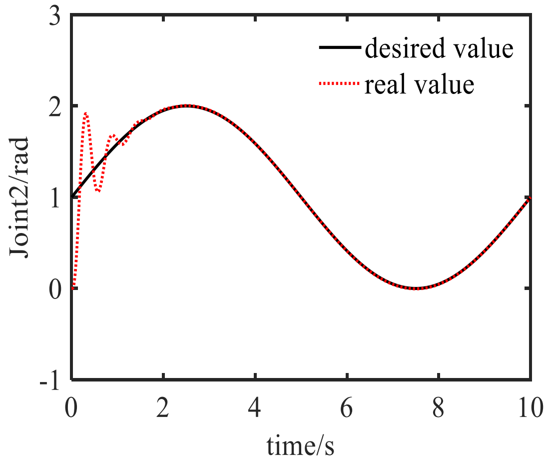

Fig.16. Joint2 angle position tracking (W-ANN)

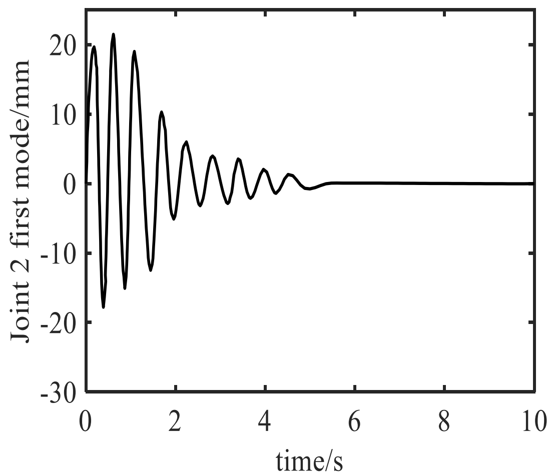

Fig.17. First order mode of flexible arm2 (W-ANN)

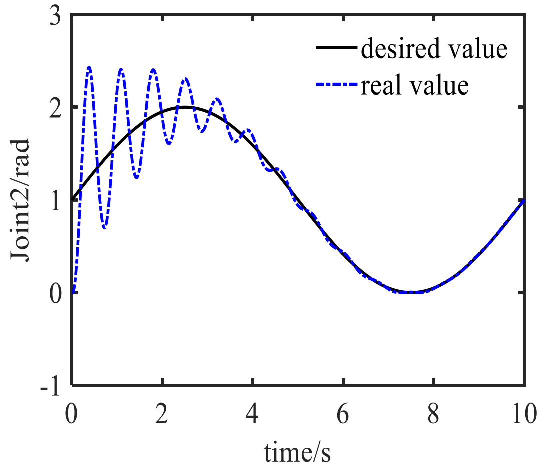

Fig.18. Joint2 angle position tracking (ANN)

From Fig.13,16 and Fig. 15,18 that the proposed two algorithms can gradually converge to the actual trajectory when the load uncertainty is $\Delta M = 2m_2 = 5kg$, which shows that the ANN algorithm is effective and still has good robustness when the load changes greatly. This shows that the ANN algorithm is effective and still has good robustness in the case of large load changes. The proposed W-ANN algorithm can accurately track the actual trajectory in about 2s (Fig.13,16). The ANN algorithm can accurately track the actual trajectory in about 5s (Fig.15,18). This shows that if the load uncertainty is large, the control performance obtained by using W-ANN algorithm is significantly better than that of ANN algorithm. Using quality estimator to estimate the unknown quality can effectively improve the control effect. From the comparison between Fig.14,17 and Fig.19,22 that when the load is uncertain, the first-order modal vibration morphology of the flexible arm is obviously aggravated, and the modal vibration mode generated by the W-ANN algorithm is better than the ANN algorithm.

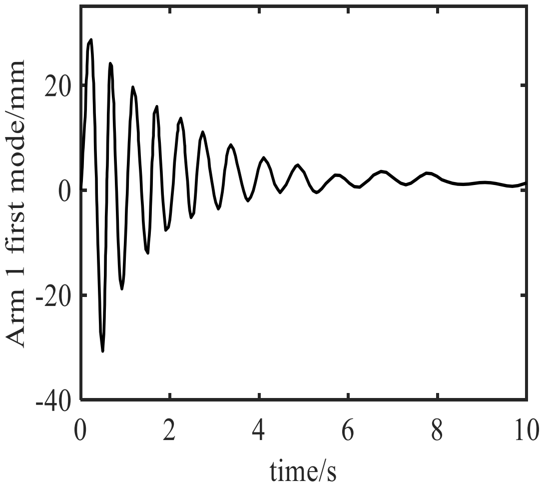

Fig.19. First order mode of flexible arm1 (ANN)

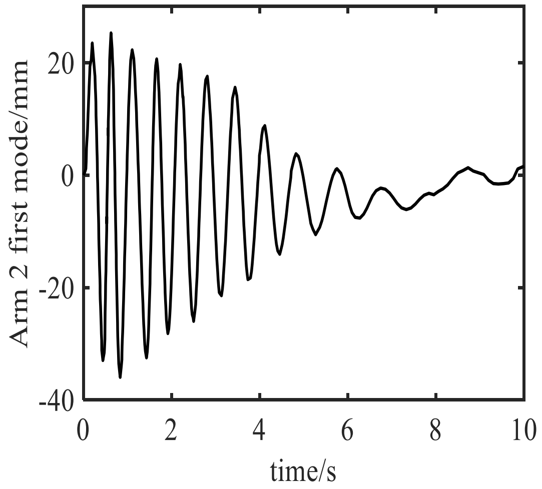

Fig.22. First order mode of flexible arm2 (ANN)

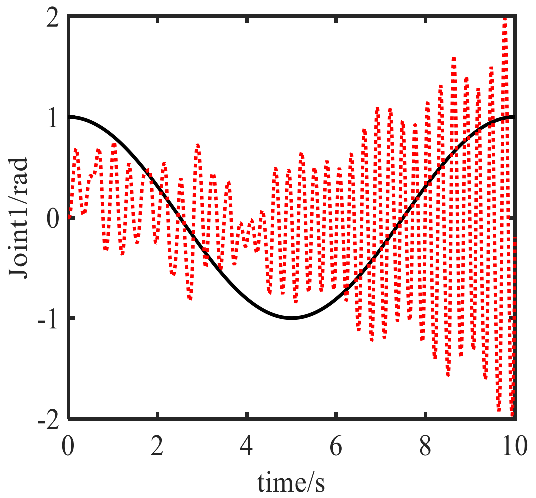

Fig.20. Joint1 angle position tracking ($\Delta M = 0.2m_2 = 0.5kg$)

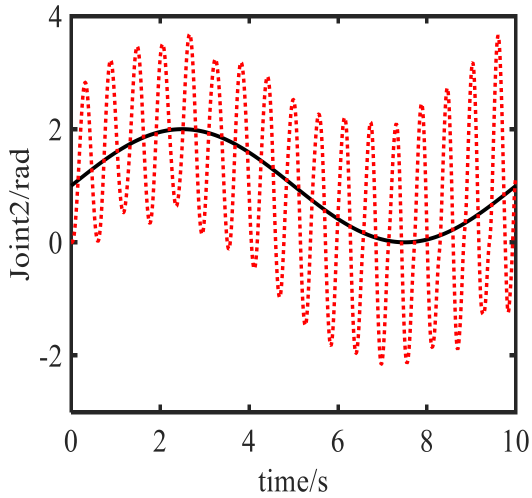

Fig.23. Joint2 angle position tracking ($\Delta M = 0.2m_2 = 0.5kg$)

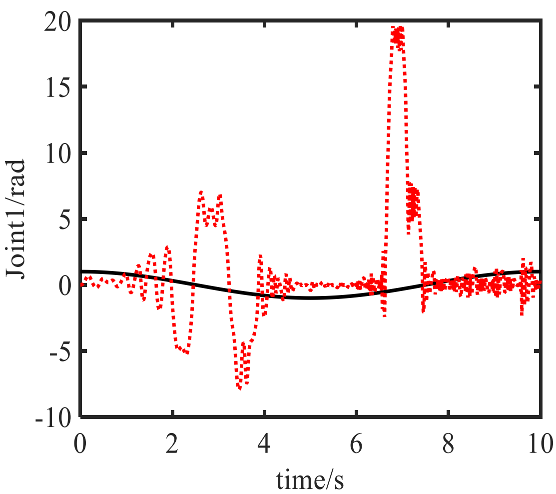

Fig.21. Joint1 angle position tracking ($\Delta M = 2m_2 = 5kg$)

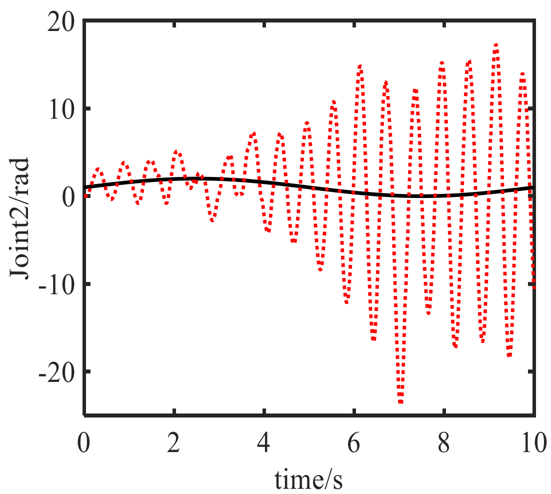

Fig.24. Joint2 angle position tracking ($\Delta M = 2m_2 = 5kg$)

D. System simulation analysis when LQR control is closed

From Fig.20,23 and Fig.21,24 , if the fast variable LQR controller is turned off, the trajectory will oscillate severely and it is completely impossible to track the upper trajectory. At the same time, it can be seen that if ΔM is larger, the oscillation is more severe.

V. CONCLUSION

A neural network control method for terminal load identification is designed to solve the variable load problem of the space robot terminal. The dynamic model of the model is decomposed into two dynamic sub models representing rigid and flexible characteristics by using singular perturbation theory. WRLSM algorithm is designed to realize identification and estimation of quality. The uncertain model error is compensated by neural network. A linear quadratic regulator (LQR) controller is designed to suppress the elastic vibration of the flexible robot. The results show that the designed controller can effectively deal with the quality change, and the control effect is effective.

REFERENCES

[1] Y. Yang, J. Shi, Z. Liu, and S. Liu, “Vibration and position tracking control for a flexible Timoshenko robot arm with disturbance rejection mechanism,” Assembly Automation, vol. 42, no. 2, pp. 248-257, 2022

[2] A. Cristofaro, A. De Luca, and L. Lanari, “Linear-Quadratic Optimal Boundary Control of a One-Link Flexible Arm,” IEEE Control Systems Letters, vol. 5, no.3, pp. 833-839, 2021.

[3] H. Jun-Pei, H. Qi, L. Yan-Hui, W. Kai, Z. Ming-Chao, and X. Zhen-Bang, “Neural Network Control of Space Manipulator Based on Dynamic Model and Disturbance Observer,” IEEE Access, vol. PP, pp. 1-1, 08/27, 2019.

[4] X. Yang, S. S. Ge, and W. He, “Dynamic modelling and adaptive robust tracking control of a space robot with two-link flexible manipulators under unknown disturbances,” International Journal of Control, vol. 91, pp. 969-988, 2018.

[5] C. Jiao, J. Yang, X. Wang, and B. Liang, “Adaptive coordinated motion control with variable forgetting factor for a dual-arm space robot in post-capture of a noncooperative target,” International Journal of Advanced Robotic Systems, vol. 16, no. 5, 2019.

[6] T. Kobayashi, and S. Tsuda, “Sliding Mode Control of Space Robot for Unknown Target Capturing,” Engineering Letters, vol. 19, no.3, pp. 105-111, 2011.

[7] J. Peng, W. Xu, E. Pan, L. Yan, B. Liang, and A.-g. Wu, “Dual-arm coordinated capturing of an unknown tumbling target based on efficient parameters estimation,” Acta Astronautica, vol. 162, pp. 589-607, 2019.

[8] D. Raina, S. Gora, D. Maheshwari, and S. V. Shah, “Impact modeling and reactionless control for post-capturing and maneuvering of orbiting objects using a multi-arm space robot,” Acta Astronautica, vol. 182, pp. 21-36, 2021/05/01/, 2021.

[9] P. Gasbarri, and A. Pisculli, “Dynamic/control interactions between flexible orbiting space-robot during grasping, docking and post-docking manoeuvres,” Acta Astronautica, vol. 110, pp. 225-238, 2015/05/01/, 2015.

[10] T. Madani, B. Daachi, and K. Djouani, “Modular-Controller-Design-Based Fast Terminal Sliding Mode for Articulated Exoskeleton Systems,” IEEE Transactions on Control Systems Technology, vol. 25, no. 3, pp. 1133-1140, 2017.

[11] A. Jouila, N. Essounbouli, K. Nouri, and A. Hamzaoui, “Robust Nonsingular Fast Terminal Sliding Mode Control in Trajectory Tracking for a Rigid Robotic Arm,” Automatic Control and Computer Sciences, vol. 53, no. 6, pp. 511-521, 2019.

[12] W. Jie, H.-H. Kim, K. Dad, and M.-C. Lee, "Terminal Sliding Mode Control with Sliding Perturbation Observer for a Hydraulic Robot Manipulator," IFAC-PapersOnLine. pp. 7-12.

[13] H. Wang, “Adaptive Control of Robot Manipulators with Uncertain Kinematics and Dynamics,” IEEE Transactions on Automatic Control, vol. 62, no. 2, pp. 948-954, 2017.

[14] W. He, Y. Chen, and Z. Yin, “Adaptive Neural Network Control of an Uncertain Robot with Full-State Constraints,” IEEE Transactions on Cybernetics, vol. 46, no. 3, pp. 620-629, 2016.

[15] M.-H. Ghajar, M. Keshmiri, and J. Bahrami, “Neural-network-based robust hybrid force/position controller for a constrained robot manipulator with uncertainties,” Transactions of the Institute of Measurement and Control, vol. 40, no. 5, pp. 1625-1636, 2018.

[16] Jia, H., Wang, J., Chen, X. et al. "H∞ Synchronization of Fuzzy Neural Networks Based on a Dynamic Event-triggered Sliding Mode Control Method," Int. J. Control Autom. Syst. vol. 20, no. 1, pp. 1882-1890, 2022.

[17] X. Zhang, J. Liu, Q. Gao, and Z. Ju, “Adaptive robust decoupling control of multi-arm space robots using time-delay estimation technique,” Nonlinear Dynamics, vol. 100, no. 3, pp. 2449-2467, 2020.

[18] X. Fu, H. Ai, and L. Chen, “Repetitive Learning Sliding Mode Stabilization Control for a Flexible-Base, Flexible-Link and Flexible-Joint Space Robot Capturing a Satellite,” Applied Sciences, vol. 11, no. 17, 2021.

[19] X. Fu, H. Ai, and L. Chen, “Integrated Fixed Time Sliding Mode Control for Motion and Vibration of Space Robot with Fully Flexible Base–Link–Joint,” Applied Sciences, vol. 11, no. 24, 2021.

[20] H. Ai, A. Zhu, J. Wang, X. Yu, and L. Chen, “Buffer Compliance Control of Space Robots Capturing a Non-Cooperative Spacecraft Based on Reinforcement Learning,” Applied Sciences, vol. 11, no. 13, 2021.

[21] A. Zhu, H. Ai, and L. Chen, “A Fuzzy Logic Reinforcement Learning Control with Spring-Damper Device for Space Robot Capturing Satellite,” Applied Sciences, vol. 12, no. 5, 2022.

[22] X. Wang, B. Xu, Y. Cheng, H. Wang, and F. Sun, “Robust Adaptive Learning Control of Space Robot for Target Capturing Using Neural Network,” 2022.

[23] C.-D. Zeng, H.-P. Ai, and L. Chen, “Collision avoidance and compliance control based on event sampling output feedback neural network for space robot dual arm capture satellite operation,” Kongzhi yu Juece/Control and Decision, vol. 36, no. 9, pp. 2113-2122, 2021.

[24] R. Lei, and L. Chen, “Adaptive neural network fault-tolerant control and residual vibration suppression for flexible-arm space robot with attitude-controlled base,” Zhendong yu Chongji/Journal of Vibration and Shock, vol. 39, no. 7, pp. 156-162, 2020.

[25] Z. Chen, and W. Jiang, “Stabilization of a constrained one-link flexible arm with boundary disturbance,” International Journal of Control, vol. 94, no. 1, pp. 134-143, 2021.

[26] F. Hamzeh Nejad, A. Fayazi, H. Ghayoumi Zadeh, H. Fatehi Marj, and S. H. HosseinNia, “Precise tip-positioning control of a single-link flexible arm using a fractional-order sliding mode controller,” JVC/Journal of Vibration and Control, vol. 26, no. 19-20, pp. 1683-1696, 2020.

[27] R.-H. Lei, and L. Chen, “Adaptive H Fault-Tolerant and Vibration-Suppressed Hybrid Control for Flexible Space ManipulatorH,” Yuhang Xuebao/Journal of Astronautics, vol. 41, no. 4, pp. 472-482, 2020.

[28] Z.-Y. Chen, and L. Chen, “Anti-torque-windup control and vibration suppression of flexible-joint dual-arm space robot with an attitude-controlled base,” Gongcheng Lixue/Engineering Mechanics, vol. 33, no. 5, pp. 227-233 and 256, 2016.

[29] E. Kang, H. Qiao, J. Gao, and W. Yang, “Neural network-based model predictive tracking control of an uncertain robotic manipulator with input constraints,” ISA Transactions, vol. 109, pp. 89-101, 2021.

[30] Y. Zheng, Y. Liu, R. Song, X. Ma, and Y. Li, “Adaptive neural control for mobile manipulator systems based on adaptive state observer,” 2022.

[31] R.-H. Lei, and L. Chen, “Finite-time tracking control and vibration suppression based on the concept of virtual control force for flexible two-link space robot,” Defence Technology, vol. 17, no. 3, pp. 874-883, 2021.